Clim. Past Discuss., 8, 557–594, 2012
www.clim-past-discuss.net/8/557/2012/
doi:10.5194/cpd-8-557-2012

Climate of the Past Discussions

Marine productivity response to Heinrich events: a model-data comparison

V. Mariotti[1], L. Bopp[1], A. Tagliabue[1,2], M. Kageyama[1], and D. Swingedouw[1]

[1]Laboratoire des Sciences du Climat et de l'Environnement, IPSL-CEA-CNRS-UVSQ, UMR8212, Centre d'Etudes de Saclay, Orme des Merisiers bat. 701, 91191 Gif Sur Yvette, France
[2]Dept. of Oceanography, Upper Campus, University of Cape Town, Cape Town, 7701, South Africa

Received: 26 January 2012 – Accepted: 30 January 2012 – Published: 14 February 2012

Correspondence to: V. Mariotti (veronique.mariotti@lsce.ipsl.fr)

Published by Copernicus Publications on behalf of the European Geosciences Union.

Abstract

Marine sediments records suggest large changes in marine productivity during glacial periods, with abrupt variations especially during the Heinrich events. Here, we study the response of marine biogeochemistry to such an event by using a biogeochemical model of the global ocean (PISCES) coupled to an ocean-atmosphere general circulation model (IPSL-CM4). We conduct a 400-yr-long transient simulation under glacial climate conditions with a freshwater forcing of 0.1 Sv applied to the North Atlantic to mimic a Heinrich event, alongside a glacial control simulation. To evaluate our numerical results, we have compiled the available marine productivity records covering Heinrich events. We find that simulated primary productivity and organic carbon export decrease globally (16 % for both) during a Heinrich event, albeit with large regional variations. In our experiments, the North Atlantic displays a significant decrease, whereas the Southern Ocean shows an increase, in agreement with paleo-productivity reconstructions. In the Equatorial Pacific, the model simulates an increase in organic matter export production but decreased biogenic silica export. This opposite behaviour results from changes in relative uptake of carbon and silicic acid by diatoms. Reasonable agreement between model and data for the large-scale response to Heinrich events gives confidence in models used to predict future centennial changes in marine production. In addition, our model enables to decipher the mechanisms behind the observed changes in the response to Heinrich events.

1 Introduction

Marine primary productivity (PP) is a key component of climate-active biogeochemical cycles such as the carbon cycle. It also sustains upper trophic levels and marine resources (Pauly and Christensen, 1995) and is the first level of marine food web impacted by climate change. The response of PP to future climate change is largely uncertain (e.g. Taucher and Oschlies, 2011) and natural variability hampers the detection

CPD
8, 557–594, 2012

of unequivocal trends from the 15-yr ocean colour satellite record (Henson et al., 2010). Coupled climate – marine biogeochemical models are used to simulate the evolution of marine PP over the historical period and under future scenarios (e.g. Steinacher et al., 2010). Such studies generally show a global decrease in PP and in the export production of organic carbon at the base of the euphotic layer (EXP) to deeper waters of between 2 and 20 % by 2100, relative to preindustrial conditions, notwithstanding regional variability in the response. A reduced input of nutrients to the euphotic zone from sub-surface waters due to increased stratification decreases PP in the North Atlantic and tropical regions, whereas lower light limitation increases Southern Ocean PP (Bopp et al., 2001; Steinacher et al., 2010). Nevertheless, evaluation of these models on such decadal-to-centennial time scales is still difficult due to sparse data covering these time scales (Schneider et al., 2008) and relatively moderate climatic change.

Turning to the geologic past, the last 100 000 yr of paleo-records may permit the evaluation of such climate-marine biogeochemical models on centennial time scales. These records show large and rapid variations linked to abrupt events such as Heinrich events (HEs) (Heinrich, 1988). During these events, massive iceberg discharges occur in the North Atlantic Ocean (Broecker et al., 1992), affecting the global ocean circulation through a collapse of the Atlantic Meridional Overturning Circulation (AMOC) (McManus et al., 2004). At the same time, there is a cooling over the North Atlantic Ocean both seen in data (Voelker, 2002; Bard et al., 2000; Cacho et al., 1999) and reproduced in climate model experiments (Kageyama et al., 2010; Swingedouw et al., 2009; Ganopolski and Rahmstorf, 2001). Alongside the climate and ocean circulation changes, ample evidence of abrupt variations in biogeochemical variables, such as EXP, are also found in marine sediments (e.g. Anderson et al., 2009; Nave et al., 2007). While paleo-records give a picture of regional processes during HEs, such as a decrease in North Atlantic EXP and an increase in the Southern Ocean, they cannot give an integrated view of the global response of marine biogeochemistry to such events due to their sparse distribution.

Biogeochemical models can provide information concerning centennial-scale marine carbon cycle dynamics. Until now, most "paleo" setting studies aimed at understanding glacial-interglacial variations of atmospheric pCO_2 observed in ice core data (Monnin et al., 2001). To explain the lower pCO_2 during glacial times compared to interglacial times, different mechanisms have been investigated, such as Southern Hemisphere westerly-wind modification (Toggweiler et al., 2006), sinking of brines (Bouttes et al., 2010), marine biology enhancement through iron fertilization (Bopp et al., 2003) or larger nutrient availability (Matsumoto et al., 2002). Alongside past CO_2 concentrations, recent models have also been used to understand changes in marine productivity between glacial and interglacial times (Kageyama et al., 2012; Oka et al., 2011; Tagliabue et al., 2009; Bopp et al., 2003). In agreement with the marine productivity compilation of Kohfeld et al. (2005), they all find a dipole effect in the Southern Ocean with enhanced EXP in the middle latitudes due to increased iron deposition and decreased EXP in the high latitudes due to increased light limitation following enhanced glacial sea-ice. The response in the other regions of the ocean are model dependent

Nonetheless, on submillennial time scales, only three model studies using Earth system models of intermediate complexity (EMICs) have investigated the response of marine biogeochemistry to HEs (Schmittner, 2005; Menviel et al., 2008; Schmittner and Galbraith, 2008). All these studies simulate a global decrease of marine productivity and a common response in certain regions (North Atlantic Ocean, Benguela coast, Mauritanian coast) matching the data, whereas in other regions they do not reproduce properly the marine response seen in data (Eastern Equatorial Pacific, Southern Ocean). These regional differences between model results and marine sediment records suggest that physical or biogeochemical processes might be missing or underestimated in these models. Such model-data mismatches need to be investigated further to understand the main mechanisms controlling key ocean regions.

Moreover, in the future, the Greenland ice sheet may melt, releasing an amount of freshwater that might resemble a HE, albeit smaller and released more to the North. The impact of such a release on the AMOC and marine biogeochemistry still remains

CPD
8, 557–594, 2012

under debate (Swingedouw et al., 2007; Schmittner et al., 2008) and validating climate models with marine biogeochemistry data from the past is clearly a key to properly evaluate the response of marine system to future freshwater input. Importantly, it is still rare that identical marine biogeochemical models are employed and tested in "paleo" settings, as well as being used for predictions of our future climate.

In this study, we investigate the global and regional response of marine biogeochemistry to a Heinrich-like event with the state of the art biogeochemical model PISCES, which has also been used for future climate projections (Steinacher et al., 2010). In a first section we present the experimental design and the comparison method performed between model and data. Then a second section details the results of the simulations both globally and regionally. A third section both discusses the discrepancies between our results and previous model studies and give some insights on potential effect of future Greenland ice sheet melting on marine biology.

2 Data compilation, model and experimental design

2.1 Data compilation

In order to evaluate our numerical results, we have compiled existing marine sediment cores documenting millenial-scale paleoproductivity changes during the past 100 000 yr.

Following Kohfeld et al. (2005) for the choice in paleoproductivity proxies, we consider either products of direct biogenic origin such as organic carbon, biogenic opal and alkenones, or indicators of biological activity such as the ratio Ba/Al or the $\delta^{13}C$ in foraminifers. Like all the species measured in marine sediments, we need to keep in mind they are subject to degradation in the water column and in the sediments, so the initial process they relate to might be slightly deteriorated.

Our compilation (Table 1) encompasses all last eight HEs and the Younger Dryas (YD). We selected only high resolution cores (with less than 500 yr between two

CPD
8, 557–594, 2012
Marine productivity response to Heinrich events: a model-data comparison
V. Mariotti et al.

measurements) in order to capture the hypothetical change in biogeochemical variables induced by a HE and get a reasonable comparison with simulations at the centennial time scale.

Because paleoproductivity is reconstructed from different proxies that are not quantitatively comparable, our method is deliberately qualitative. We associate to each record a sign for productivity changes during HEs and a degree of confidence which are a combination of the trend of the proxies, the number of proxies and the number of documented events. The details of our method can be found in Table 1. We end up with 49 data points that are gathered in Fig. 1 and will be discussed later.

2.2 The biogeochemical model PISCES

The Pelagic Interaction Scheme for Carbon and Ecosystem Studies (PISCES) marine biogeochemical model includes a simple representation of marine ecosystem and of main biogeochemical cycles and is composed of 24 pools in total. Among them, there are two size classes of phytoplankton (nanophytoplankton and diatoms), two size classes of zooplankton, five pools of nutrients (phosphate, ammonium, nitrate, silicic acid, iron), small and large particulate-organic-carbon, one of dissolved-organic-carbon and another one of dissolved-inorganic-carbon. These pools interact with each other following the main biogeochemical processes such as photosynthesis, respiration, grazing, particle aggregation, particle sinking, remineralisation and sedimentation (for more details on the model, see Aumont and Bopp, 2006). Phytoplankton growth in the model is limited by five nutrients (nitrate, phosphate, ammonium, silicic acid, iron), by light availability (a function of photosynthetically active radiation reaching the ocean surface, the optical properties of the water and the mixed-layer depth). The ratios for C/N/P are kept constant following Redfield ratios. However, the ratio of silica and iron to carbon in phytoplankton biomass varies in function of nutrient availability and light. For instance, following culture experiments (Hutchins and Bruland, 1998; Takeda, 1998), the ratio of silica to carbon in diatom cells is modulated by the degree of Fe limitation making diatoms more silicified under more severe Fe limitation.

CPD
8, 557–594, 2012

The model has already been evaluated under glacial conditions (Tagliabue et al., 2009; Bopp et al., 2003) and reproduces roughly the paleoproductivity reconstruction of Kohfeld et al. (2005). One of the more consistent patterns is a dipole effect in the Southern Ocean with enhanced EXP in the middle latitudes due to increased iron deposition and decreased EXP in the high latitudes due to increased light limitation following enhanced glacial sea-ice.

2.3 Experimental design

PISCES is forced offline by the atmosphere-ocean general circulation model IPSL-CM4 (Marti et al., 2010), which includes the ocean dynamical model NEMO with $2^\circ \times 2^\circ - 0.5^\circ$ horizontal resolution and 31 vertical levels, 10 being located in the first 100 m.

Two 400-yr-experiments have been performed under Last Glacial Maximum (LGM) conditions, with the orbital parameters, greenhouse gas concentrations and ice sheets from 21 000 yr before present (see Kageyama et al., 2009, for a detailed presentation of the climate setup). The biogeochemical simulations based on these experiments use a constant atmospheric CO_2 concentration fixed at LGM level (190 ppm) and constant LGM dust deposition distribution (Mahowald et al., 2006), which is important for aeolian iron interaction with marine biology. The first experiment is an equilibrated glacial run (GLA) used as a reference run. The second experiment is a hosing experiment (FWF), starting from year 100 of the reference run. In this experiment, the freshwater implemented in the reference run to balance snow accumulating on the ice sheets is multiplied by 2.27. This results in an additional freshwater flux of 0.1 Sv (1 Sverdrup = $10^6\ m^3\ s^{-1}$) in the Atlantic North of 40° N and the Arctic, which mimics the icebergs melting during an HE. In FWF simulation, the AMOC collapses in around 250 yr. This is a relatively long time response compared to the simulation time but a relatively short time response compared to the resolution of most of the marine records. Indeed these records do not allow to distinguish if the changes in the AMOC happened within 10 or 400 yr.

CPD
8, 557–594, 2012

For this study, we only focus on the biogeochemical results of these simulations. The ocean atmosphere dynamics results of these simulations are analysed in details in Kageyama et al. (2009).

We first study EXP as it is clearly more relevant to be compared with sediment core observations. But, as Taucher and Oschlies (2011) have pointed out for projection simulations, there might be cases where the response of PP and EXP to climate can be decoupled, so we will examine these results once the fidelity of the model performance has been assessed.

In the following, we define a typical Heinrich-like event in the model through the difference between the FWF and GLA simulations averaged over the last 50 yr of the simulations. We will compare such a signature with our data compilation, where the weighted mean of the 9 events is considered to represent a typical HE in the observations.

3 Results

3.1 Statistical match between model and data

In total, we found 49 marine records studies capturing at least one HE (or YD). In short, 26 record a decrease in EXP during this period, while 14 show an increase and 9 do not provide a significant trend (Table 1). If we consider the 40 records that display a significant trend, the model outputs match 26 of these cores (Fig. 1). Among the 14 model-data mismatches, 6 of the data points (ODP882, Core 17950-2, GeoB3302-1, GeoB3359-3, TN057-13-4PC and NBP9802-6PC, see Table 1 for precise location) are located on a model front area. PISCES does represent the main features of nutrients distribution, but some fronts can be shifted a little bit, due to the biases of the model, so this could explain part of the mismatches. Four of the data points (MD02-2519, MD02-2524, MD02-2529 and GeoB7139-2) are located in an area where the model does not simulate a significant change in EXP (between −1 and 1 $gC\,m^{-2}\,yr^{-1}$). One data point (PL07-57PC) is displaying an increase in EXP while two other data points (M35003-4

Discussion Paper | Discussion Paper | Discussion Paper | Discussion Paper |
CPD
8, 557–594, 2012
Marine productivity response to Heinrich events: a model-data comparison
V. Mariotti et al.

and PL07-29PC) within the same area display a decrease in EXP just as the model does. This last point raises the problem of comparing local data points to regionally averaged model cells. Even if we consider that the signal captured by marine cores has been well preserved within both the water column and the sediments, each data record is nonetheless the addition of a regional signal and a local signal. The model simulates only the regional part of the signal, and we would need several data points for one cell of the model to be entirely confident with the statistical comparison. The 3 last points (MD04-2805 CQ, GeoB5546-2 and GeoB7925-2) are located on the Mauritanian coast and are clearly in contradiction with the model results. We will discuss in more details the results for this region in the following section. Nevertheless, if we consider cores where the model matches the sediment record at almost the same location (including the cores in front areas), we match the sign of the response of EXP in 80 % of places. Hence, our model seems to be able to simulate the main response of EXP to HEs correctly, or at least its first order mechanisms.

3.2 Regional analysis

In order to use our model-data comparison to better understand the response of EXP in key regions, we define a few box regions (Fig. 1 and Table 2). We first focus on regions where proxy data is available: either model and data are in agreement as in NATL, BEN, EEP and IND, or there is a clear contradiction as in MAU. In addition, we also specifically focus on the Southern Ocean, because of its major contribution to global EXP and because of the meridionally diverse response of PP to HEs in that region.

3.2.1 North Atlantic

The North Atlantic (NATL, see Table 2 for description of the precise location) is the region where most of the marine records are located (15 in total, 11 with significant trends, see Table 1) and our modelled Heinrich-like event matches the sign of all the significant records. In the model, a decreasing winter mixed-layer depth (by more than

CPD
8, 557–594, 2012

150 m in February, Fig. 2a) reduces the nutrient flux to the upper ocean (not shown). Moreover, an increasing sea ice cover (Fig. 2b) reduces light availability. Both these processes cause a decrease in EXP of 44 % (Table 2).

Gil et al. (2009) find an increase in EXP at core OCE326GGC6, located south of the present day Gulf Stream. Their data did not pass our test for significant data because the duration of their record before HE1 was less than 3000 yr, limiting the comparison to a glacial state. Nonetheless, they explain this increase in EXP by an iceberg migration to the subtropics inducing an isolated environment involving turbulent mixing, upwelled water and nutrient-rich meltwater supporting productivity. This hypothesis has not been tested in our model set-up and could not be confirmed or dismissed because (1) we do not have enough horizontal resolution to account for meso-scale processes and (2) we do not take into account nutrient input accompanying freshwater discharge.

Overall, our model matches the reduction in EXP during HEs in the North Atlantic in most cases and we suggest that the response results from greater limitation of PP and thus also of EXP by both nutrients and light.

3.2.2 Southern Ocean

In the Southern Ocean, there are 4 records indicating an increase of EXP (MD97-2120, TN057-13-14PC, E27-23, NBP9802-6PC). Our simulations match these 4 records but the response of the model shows significant zonal variability. We therefore focus here on two regions of interest that illustrate the major trends: an area in the South-East of New-Zealand (NZL) and an area in the South-East Pacific (SEP).

In the NZL area, South of the Polar Front, our model simulates a 6.4 % increase in EXP (Table 2) in agreement with two different sediment cores from this same area (E27-23, NBP9802-6PC). The model suggests that a deepening of the winter mixed-layer depth, combined with a strengthening of the upwelling, act together to increase the nutrient flux to the euphotic zone and stimulate PP and EXP. In particular, we note enhanced input of silicic acid in FWF compared to GLA (see Fig. 3) as suggested by Anderson et al. (2009). In the model, this input is due to enhanced simulated westerlies (increase of 1 m s^{-1} between 55° S and 60° S; Fig. 3).

CPD
8, 557–594, 2012

In the SEP area, EXP decreases by 17 % in the model (Table 2), in contrast to the NZL region. Our model simulates increasing winter sea-ice that isolates the surface waters from the atmosphere in this area. This "barrier effect" of sea ice means that winds cannot deepen the winter mixed layer enough to introduce nutrients in the upper ocean, which would be available for consumption by phytoplankton in spring. Moreover, greater sea ice also reduces the springtime light availability. Both these processes (reduced winter mixing and less springtime irradiance) induce a decrease in EXP in this area. As far as we know, no paleo-productivity proxy with millennial scale resolution has been published in this area, so we cannot compare our results with any data. We found one sediment core (E11-2 in Mashiotta et al., 1999) displaying SST reconstructions for the last deglaciation and HE1 but this record does not have a substantial decrease in surface temperature that would expect to be associated with an enhanced sea ice. On the contrary, SST generally increases from the LGM to the Holocene in this region. Some global climate models also find this SST anomaly in the SEP, but others do not (Kageyama et al., 2009, 2010; Merkel et al., 2010; Otto-Bliesner and Brady, 2010), so this pattern could be model dependent. We need further high resolution data to discriminate between model results and better understand the main processes involved in this area.

Overall, our model matches the increased EXP noted in the sediment cores in the Southern Ocean, but we highlight a large degree of spatial variability in the response of EXP to different patterns of winter mixing and sea ice.

3.2.3 East Equatorial Pacific

In the East Equatorial Pacific (EEP), 5 cores (3 cores with a significant trend) are available at almost the same location (they appear as one red point in Fig. 1) and indicate a 2 % increase in EXP (Table 2). The model also simulates an increase in EXP, which is the result of greater equatorial upwelling due to stronger trade winds alongside a deepening of the mixed-layer depth. Both mechanisms increase the nutrient availability in this area and agree with concomitant decreased reconstructed SST and increased

CPD
8, 557–594, 2012

organic carbon content in sediment (Kienast et al., 2006). Although the model simulates an increase in EXP (Fig. 4d), it shows a simultaneous decrease in the export of silicate (Fig. 4c), a biomarker for diatoms, which might appear counter-intuitive. However, laboratory data has shown that when diatoms are iron limited, they adapt to this new environment consuming more silicate relative to C and N (Hutchins and Bruland, 1998; Takeda, 1998) thereby allowing the export of Si and C to become decoupled; this process is included in our model. In the context of HEs, the exact contrary happens, with diatoms experiencing greater iron availability, which decreases their relative silicic acid uptake and decreases the Si/C ratio for diatoms (Fig. 4b). This process drives a decrease in the export of silicate, even if EXP increases. This process has already been pointed out by Pichevin et al. (2009) at site ODP 1240 (see Table 1) for glacial/interglacial time-scales and our simulations reveal that it seems to be a critical process on submillennial time-scales as well (see Fig. 4). The EEP is in fact a High Nutrient-Low Chlorophyll (HLNC) region, which is iron-limited, so variation in the input of iron can induce high variations in EXP. As for the origin of iron, Leduc et al. (2007) showed that during HEs, the southward shift of the Inter Tropical Convergence Zone (ITCZ) can induce drier air that conveys more airborne iron. In our model, the airborne iron flux is kept constant at glacial levels between the two simulations, so we cannot capture this effect. Nevertheless, the model simulates greater iron supply to EEP surface waters due to enhanced vertical supply. Subsurface ocean is clearly to be considered as a potential source for iron during HEs in this region. It is encouraging that our model reproduces the trend of EXP recorded in proxies, as well as capturing the decoupling between the export of carbon and silica noted in the geologic record in EEP.

3.2.4 Coastal regions

Coastal regions are not the best areas to test our model results as the model cannot capture specific coastal processes because of its coarse resolution. These areas are nevertheless regions where most data are available because of an important

CPD
8, 557–594, 2012

sedimentation rate which allows a high-resolution analysis, so we endeavour to examine them. Our assumption is that the main signature found in coastal area is related to large-scale changes.

Three proxy-based studies are available on the Mauritanian coast (MAU); they all find increased EXP in response to HEs linked to an enhanced upwelling (Penaud et al., 2010; Holzwarth et al., 2010; Romero et al., 2008). However, in contrast to these records, our runs simulate a 58 % decrease in EXP (Table 2). We do observe an enhanced upwelling in our simulations (not shown) but it is completely offset by the overall thinning of the mixed layer induced by the freshwater forcing in North Atlantic. It is plausible that our idealised freshwater forcing might be too strong compared to real HEs or that the zone of freshwater input does not exactly correspond to the region where icebergs melt.

On the Benguela coast (BEN), EXP decreases both in data (GeoB1706-2, GeoB1711-4, GeoB3606-1) and in the model (by 66 %, Table 2). In the mean glacial state, there is an important upwelling in this area that decreases significantly during our HE experiment. Therefore most of nutrient enriched sub-surface waters do not reach the euphotic layer, which reduces EXP by increasing nutrient limitation.

In the Indian Ocean (IND), more precisely in the Arabian Sea, the model simulates decreased EXP (by 47 %, Table 2), in good agreement with high resolution data (Ivanochko et al., 2005; Schulte and Müller, 2001). In this region, EXP is primarily controlled by upwellings, themselves induced by monsoon westerlies (Bassinot et al., 2011). Kageyama et al. (2009) found a weaker monsoon in the Heinrich-like event simulation we use. This weaker monsoon thus induces weaker upwellings and then decreased EXP.

Overall, despite the potential problems in comparing global model results to coastal sediment cores, our model succeeds in reproducing the observed trends in the BEN and IND regions. We suppose that the mismatch in the MAU region could be due to the highly idealised way in which we simulate HEs.

3.3 Global analysis

When globally integrated, EXP decreases by 16 %, or 1.5 Pg (Table 2 and Fig. 5d) by the end of the simulations, in response to a HE. This decrease occurs in parallel to an 87 % (or 13 Sv) reduction in the strength of the AMOC as induced by the constant freshwater flux applied into North Atlantic (Fig. 5a). EXP depends on nutrients, and the nutrient availability itself is highly dependent on nutrient supply through ocean ventilation and mixing. The constant freshwater flux that we use to approximate a HE induces an increase in the degree of stratification (shown by a decreased Northern Hemisphere winter mixed layer depth Fig. 5b), especially in the North Atlantic where the signal is the most important. This increased stratification leads to a decrease in the ventilation of the subsurface ocean and thus to a decrease of nutrient supply (cf. the decrease of almost 13 % of global nitrate concentration at the surface in Fig. 5c). This explains the global decrease in EXP. We note that whereas the AMOC stabilises at around 2 Sv by the end of our simulation, EXP continues to decrease linearly over the entire 400 yr period.

As explained in the experimental design section, we have chosen to compare our modeled EXP to available marine productivity data, making the hypothesis that PP and EXP are varying in the same direction. However, Taucher and Oschlies (2011) recently showed that it is not always the case in response to climate variability. When the temperature increases, metabolic effects cause an increase in both PP and remineralisation of organic matter by bacteria. Greater remineralisation can reduce EXP, but may also yield positive feedback on PP via the subsequent increase in available renewed nutrients due to greater heterotrophy. In order to investigate if PP and EXP respond similarly in our experiment, we plot the ratio of the comparative change in these two quantities in Fig. 6. We can see that for the areas we studied (Fig. 1) PP and EXP vary in the same direction, so our modeled EXP is a correct “proxy” of PP in these areas. Alternatively, there are some regions where the model simulates opposite responses for PP and EXP. Most of these areas are located in the boundary between an increased

CPD
8, 557–594, 2012

and a decreased EXP so they are probably due to horizontal advection effects. We can note that the ones located in the Southern Hemisphere correspond to regions showing an increase in temperature (Fig. 6). Taucher and Oschlies's hypothesis can thus partly explain the differences observed between PP and EXP (the parameterization of PP and remineralisation is indeed dependent on temperature in PISCES).

4 Discussion

4.1 Comparison with other model studies

Other model studies (Menviel et al., 2008; Schmittner, 2005) have examined the response of EXP to freshwater forcing with models of intermediate complexity. The freshening scenarios applied were different from those employed in this study, so we cannot compare the results quantitatively, as explained by Bouttes et al. (2011) who discuss on different hosing scenarios in generating Heinrich events and how they impact on the ocean carbon cycle. We can however qualitatively examine the patterns in the EXP response between models.

In general, the reduced EXP in NATL and BEN are consistent between the models suggesting that these are robust responses to freshwater fluxes input in the North Atlantic. However, there are regions where the models have a different response to hosing. We will focus on EEP, NZL, MAU and IND. These are regions where EXP is mainly controlled by upwelling. As coarse-resolution climate models usually have difficulties to simulate upwellings correctly, we first check that upwellings are well represented in the modern version of each model before drawing any conclusion on glacial centennial-scale changes in these regions. The IPSL-CM4 model does represent all these upwellings (Bassinot et al., 2011; Steinacher et al., 2010; Lenton et al., 2009; Schneider et al., 2008) though it tends to underestimate their intensity both in terms of upwelled water flux and surface productivity. The LOVECLIM model represents the EEP and NZL upwellings but not the MAU and IND ones (see Menviel et al., 2008,

CPD
8, 557–594, 2012

Figs. 5 and 6). The UVic model represents the EEP, NZL and IND upwellings, but not the MAU one (see Schmittner, 2005, Figs. 2 and 3). We need also to point out that while Menviel et al.'s simulations and our simulations are performed with interactive winds, Schmittner's simulations use prescribed modern winds, so his simulations cannot capture wind-driven changes in upwellings.

In EEP and most of the Southern Ocean we find an increased EXP which is in contrast to both previous model studies. For both regions, we attribute this difference to the wind-driven increased upwelling. We explain the difference with Schmittner's study by his non representation of winds changes. For Menviel et al.'s study that does represent these upwelling areas in modern times and computes wind changes, we hypothesize that the discrepancies between our models are probably due to two factors. On one hand, our model has an increased atmospheric resolution, so we hypothesize it captures better the wind changes in upwelling areas. On the other hand, our model has a parameterization of Si/C as a function of temperature and iron availability that is not implemented in LOVECLIM and we have shown in the results section that this parameterization was key to simulate the EEP region changes.

In IND, our study finds a decrease in EXP due to an enhanced upwelling as does Schmittner (2005) whereas Menviel et al. (2008) simulate an increase in EXP. As Schmittner's simulations have prescribed preindustrial winds, he claims that the decrease in upwelling seen in his simulations is thermohaline-driven. As explained above, the modern simulations of LOVECLIM do not represent the upwelling in this area, so it cannot obviously simulate changes of upwelling regimes in this area.

In MAU, the decreased EXP we simulate is at odds with both data and previous model studies which present an increased EXP due to an enhanced upwelling. We need to explain why our model, supposed to be able to capture changes in wind-driven upwellings, is not able to capture the signal of increased productivity seen in data. We make the hypothesis that it is due to the location of our hosing. The hosing is applied between 40° N and 90° N in our experiment, which is South enough to make the freshwater being advected through the subtropical gyre directly to the Mauritanian coast. On the contrary, in the other studies, the hosing is applied more northward (between 50° N and 65° N for Menviel et al., 2008, and between 45° N and 65° N for Schmittner, 2005), which makes the freshwater flow northward through the North Atlantic Current. Hence, the surface waters are considerably mixed through the subpolar gyre before they arrive on the Mauritanian coast. We do have an increase of upward vertical velocities in the upper ocean of this region (not shown), but this increased upwelling is completely balanced by the freswater lid that does not allow the nutrients to spread out from the subsurface waters. In addition, the modern simulations previously performed with our model (Steinacher et al., 2010) display a really weak upwelling in this area compared to data, so this underestimation of vertical velocities can explain why it cannot balance the lid effect. Nonetheless, the other studies simulate an increase in productivity in MAU whereas it cannot be explained by an enhanced upwelling as they propose. Their models both simulate a decrease in the utilization of nutrients in the upper latitudes of the North Atlantic Ocean due to the freshwater induced stratification. We hypothesize that this might lead to an increase of subsurface water nutrients in the North Atlantic Ocean that are advected southward into MAU. To summarize, in MAU, according to data, there was an enhanced upwelling during HEs inducing increased EXP, but our model cannot reproduce it because of (1) a too weak intensity of the upwelling in modern times and (2) a freshwater forcing too close to the upwelling area.

In conclusion, the differences between model results come mostly from atmospheric resolution and nutrient parameterization differences but also from the different locations of freshwater forcing and the way the models advect them from the area of freshening. Overall, except for the Mauritanian coast, our study correctly simulates the response of EXP to HEs, and points out the importance of the Si/C ratio parameterization in marine biogeochemical models.

4.2 What do these results tell us for 21st century projections?

We do not have yet any certainty on the sign of the global evolution of marine PP with global warming (Taucher and Oschlies, 2011). Investigating the response of marine

CPD
8, 557–594, 2012

biogeochemical models to HEs could be of use in examining the predicted impact of climate change on marine biogeochemistry. Valdes (2011) recently pointed out that the coupled climate models might be too stable to simulate abrupt centennial scale changes like the actual global warming and that they need to be tested on past abrupt climate changes. This study shows that the model IPSL-CM4 including PISCES is able to represent the main features of EXP response to a HE. With the sediment data currently available, we are not able to test if the model answers quantitatively well. We need further more attempts of PP or EXP calibration from different biomarkers as it has been done by Salgueiro et al. (2010) or Beaufort et al. (1997) to have a more direct comparison with our model outputs. Nonetheless, the model can simulate an EXP response to HEs qualitatively consistent with available data, and more importantly with a fast time response in certain regions, like in the Atlantic Ocean which responds strongly within a hundred years (see Fig. 7). Even with an AMOC decreasing on slower timescales (≃250 yr), PISCES model forced by IPSL-CM4 output seems to be able to simulate transient climate changes on centennial scale. This is encouraging as it has been used for climate projections. Nonetheless, we need to point out that while our model simulates a global decrease of PP by 16 % with HEs, we still do not have any global constrain to validate this result. New isotopic methods using for instance the triple isotopes (Landais et al., 2007) or the Dole effect (Landais et al., 2010) should be used to investigate this result. Simulating HEs could be a benchmark for coupled climate carbon cycle models to test their ability to simulate abrupt transient climate changes, and our compilation of paleoproductivity proxies could be used to compare the results of the models to available data.

Studying the response of EXP to HEs can also give insights of mechanisms that may affect EXP under global warming. The radiative effect of increased CO_2 and subsequent warming on marine biology has already been tested. Steinacher et al. (2010) performed a model inter-comparison between four coupled climate-carbon cycle models for future climate. Significant regional differences between the models in the response of EXP to climate change appear but there are shared patterns like a decrease

Discussion Paper | Discussion Paper | Discussion Paper | Discussion Paper |
CPD
8, 557–594, 2012
Marine productivity response to Heinrich events: a model-data comparison
V. Mariotti et al.

of EXP in NATL and an increase in the Southern Ocean. Global warming is also accompanied by a melting of the Greenland ice sheet which is not taken into account in most of the actual coupled models. Our study could represent an analogue to this future Greenland melting which is implemented in the study of Steinacher et al. (2010) only for one model (IPSL-CM4) out of four models. Of course our study starts with a glacial climate background so this could induce differences in the intensity of the response of the system compared to the same freshwater forcing with an interglacial climate background, so we need to be careful when comparing our HEs simulations with global warming freshwater forcing projections. Nonetheless we can point out some significant trends, like a decrease of EXP in the North Atlantic, a region that is already projected to undergo a decrease of EXP due to global warming. This result is in agreement with the fact that the IPSL model in Steinacher et al. (2010) study was already simulating a more important decrease in this region. Hence, actual projections may underestimate the decrease of EXP in this region. Swartz et al. (2010) have shown that actual increased fishing induces a higher percentage of required PP to sustain global fish populations, with a special increase in North Atlantic Ocean. Projections including a freshwater forcing may be of use to help constraining EXP response in the future, especially for the areas of actual intense fishing that could be strongly affected in the coming decades.

5 Conclusions

This study first aimed at evaluating the response of a marine biogeochemistry model (PISCES) to centennial scale events in glacial times, using marine cores for comparison. The model results regarding the response of marine biology to Heinrich events are most of the time qualitatively consistent with paleo-data, which is encouraging for its ability to simulate future climate impacts on primary productivity and especially abrupt centennial scale changes. The data compilation for paleoproductivity we gathered and used to test our model results can be used as a tool to evaluate other coupled

CPD
8, 557–594, 2012

Marine productivity response to Heinrich events: a model-data comparison

V. Mariotti et al.

biogeochemical-climate models response to Heinrich events and their ability to simulate a centennial scale climate change. Our work also highlights the importance of the Si/C ratio parameterization in models as a key mechanism to simulate certain regions ecosystem, here in the Eastern Equatorial Pacific. This study also points out the importance of multi-proxy analysis to interpret paleoproductivity in the sediments.

The second aim of this study was to use the model to more accurately understand the global and regional response of marine productivity to Heinrich events. We simulate a global decrease of primary productivity of 16 % following the freshwater forcing, with some regional differences. According to our data-model intercomparison, it is very likely that the North Atlantic Ocean, the south-western coast of Africa and the Indian Ocean experienced a decrease in primary productivity, whereas the Southern Ocean and the Eastern Equatorial Pacific experienced an increase during Heinrich events. This study gives us also an insight of what could be the contribution of a melting of Greenland ice sheet in the coming century: an accentuated decrease of organic matter export in the North Atlantic Ocean.

Supplementary material related to this article is available online at: http://www.clim-past-discuss.net/8/557/2012/cpd-8-557-2012-supplement.pdf.

Acknowledgements. We thank the French National Computing Center CEA/CCRT for the computer time provided.

The publication of this article is financed by CNRS-INSU.

References

Anderson, R., Ali, S., Bradtmiller, L., Nielsen, S., Fleisher, M., Anderson, B., and Burckle, L.: Wind-driven upwelling in the Southern Ocean and the deglacial rise in atmospheric CO_2, Science, 323, 1443–1448, doi:10.1126/science.1167441, 2009. 559, 566, 586

Arellano-Torres, E., Pichevin, L., and Ganeshram, R.: High-resolution opal records from the eastern tropical Pacific provide evidence for silicic acid leakage from HNLC regions during glacial periods, Quaternary Sci. Rev., 30, 1112–1121, doi:10.1016/j.quascirev.2011.02.002, 2011. 586

Aumont, O. and Bopp, L.: Globalizing results from ocean in situ iron fertilization studies, Global Biogeochem. Cy., 20, doi:10.1029/2005GB002591, 2006. 562

Bard, E., Rostek, F., Turon, J., and Gendreau, S.: Hydrological impact of Heinrich events in the subtropical northeast Atlantic, Science, 289, 1321–1324, doi:10.1126/science.289.5483.1321, 2000. 559

Bassinot, F. C., Marzin, C., Braconnot, P., Marti, O., Mathien-Blard, E., Lombard, F., and Bopp, L.: Holocene evolution of summer winds and marine productivity in the tropical Indian Ocean in response to insolation forcing: data-model comparison, Clim. Past, 7, 815–829, doi:10.5194/cp-7-815-2011, 2011. 569, 571

Beaufort, L., Lancelot, Y., Camberlin, P., Cayre, O., Vincent, E., Bassinot, F., and Labeyrie, L.: Insolation cycles as a major control of equatorial Indian Ocean primary production, Science, 278, 1451–1454, doi:10.1126/science.278.5342.1451, 1997. 574

Bopp, L., Monfray, P., Aumont, O., Dufresne, J., Le Treut, H., Madec, G., Terray, L., and Orr, J.: Potential impact of climate change on marine export production, Global Biogeochem. Cy., 15, 81–99, doi:10.1034/j.1600-0889.2003.042.x, 2001. 559

Bopp, L., Kohfeld, K., Le Quere, C., and Aumont, O.: Dust impact on marine biota and atmospheric CO_2 during glacial periods, Paleoceanography, 18, 1046, doi:10.1029/2002PA000810, 2003. 560, 563

Bouttes, N., Paillard, D., and Roche, D. M.: Impact of brine-induced stratification on the glacial carbon cycle, Clim. Past, 6, 575–589, doi:10.5194/cp-6-575-2010, 2010. 560

Bouttes, N., Roche, D. M., and Paillard, D.: Systematic study of the fresh water fluxes impact on the carbon cycle, Clim. Past Discuss., 7, 1363–1392, doi:10.5194/cpd-7-1363-2011, 2011. 571

Broecker, W., Bond, G., Klas, M., Clark, E., and McManus, J.: Origin of the northern Atlantic's Heinrich events, Clim. Dynam., 6, 265–273, 1992. 559

Cacho, I., Grimalt, J., Pelejero, C., Canals, M., Sierro, F., Abel Flores, J., and Shackleton, N.: Dansgaard-Oeschger and Heinrich event imprints in Alboran Sea paleotemperatures, Paleoceanography, 14, 698–705, 1999. 559

Calvo, E., Pelejero, C., Pena, L., Cacho, I., and Logan, G.: Eastern Equatorial Pacific productivity and related-CO_2 changes since the last glacial period, P. Natl. Acad. Sci., 108, 5537–5541, doi:10.1073/pnas.1009761108, 2011. 586

Dean, W. E.: Sediment geochemical records of productivity and oxygen depletion along the margin of western North America during the past 60,000 years: teleconnections with Greenland Ice and the Cariaco Basin, Quaternary Sci. Rev., 26, 98–114, doi:10.1016/j.quascirev.2006.08.006, 2007. 585, 586

Dubois, N., Kienast, M., Kienast, S., Normandeau, C., Calvert, S. E., Herbert, T. D., and Mix, A.: Millennial-scale variations in hydrography and biogeochemistry in the Eastern Equatorial Pacific over the last 100 kyr, Quaternary Sci. Rev., 30, 210–223, doi:10.1016/j.quascirev.2010.10.012, 2011. 586

Galbraith, E., Jaccard, S., Pedersen, T., Sigman, D., Haug, G., Cook, M., Southon, J., and Francois, R.: Carbon dioxide release from the North Pacific abyss during the last deglaciation, Nature, 449, 890–893, doi:10.1038/nature06227, 2007. 586

Ganopolski, A. and Rahmstorf, S.: Rapid changes of glacial climate simulated in a coupled climate model, Nature, 409, 153–158, 2001. 559

Gil, I., Keigwin, L., and Abrantes, F.: Deglacial diatom productivity and surface ocean properties over the Bermuda Rise, northeast Sargasso Sea, Paleoceanography, 24, PA4101, doi:10.1029/2008PA001729, 2009. 566, 585

Heinrich, H.: Origin and Consequences of Cyclic Ice Rafting in the Northeast Atlantic Ocean during the Past 130,000 Years, Quaternary Res., 29, 142–152, doi:10.1016/0033-5894(88)90057-9, 1988. 559

Henson, S. A., Sarmiento, J. L., Dunne, J. P., Bopp, L., Lima, I., Doney, S. C., John, J., and Beaulieu, C.: Detection of anthropogenic climate change in satellite records of ocean chlorophyll and productivity, Biogeosciences, 7, 621–640, doi:10.5194/bg-7-621-2010, 2010. 559

Holzwarth, U., Meggers, H., Esper, O., Kuhlmann, H., Freudenthal, T., Hensen, C., and Zonneveld, K.: NW African climate variations during the last 47,000 years: Evidence from organic-walled dinoflagellate cysts, Palaeogeogr. Palaeocl., 291, 443–455, 2010. 569, 585

Hughen, K., Overpeck, J., Peterson, L., and Trumbore, S.: Rapid climate changes in the tropical Atlantic region during the last deglaciation, Nature, 380, 51–54, 1996. 585

Hutchins, D. and Bruland, K.: Iron-limited diatom growth and Si: N uptake ratios in a coastal upwelling regime, Nature, 393, 561–564, 1998. 562, 568

Ivanochko, T., Ganeshram, R., Brummer, G., Ganssen, G., Jung, S., Moreton, S., and Kroon, D.: Variations in tropical convection as an amplifier of global climate change at the millennial scale, Earth Planet. Sc. Lett., 235, 302–314, doi:10.1016/j.epsl.2005.04.002, 2005. 569, 586

Kageyama, M., Mignot, J., Swingedouw, D., Marzin, C., Alkama, R., and Marti, O.: Glacial climate sensitivity to different states of the Atlantic Meridional Overturning Circulation: results from the IPSL model, Clim. Past, 5, 551–570, doi:10.5194/cp-5-551-2009, 2009. 563, 564, 567, 569

Kageyama, M., Paul, A., Roche, D., and Van Meerbeeck, C.: Modelling glacial climatic millennial-scale variability related to changes in the Atlantic meridional overturning circulation: a review, Quaternary Sci. Rev., 29, 2931–2956, 2010. 559, 567

Kageyama, M., Braconnot, P., Bopp, L., Caubel, A., Foujols, M.-A., Guilyardi, E., Khodri, M., Lloyd, J., Lombard, F., Mariotti, V., Marti, O., Roy, T., and Woillez, M.-N.: Mid-Holocene and Last Glacial Maximum climate simulations with the IPSL model: new features with the IPSL CM-5A version, submitted to Clim. Dynam., 2012. 560

Kienast, S., Calvert, S., and Pedersen, T.: Nitrogen isotope and productivity variations along the northeast Pacific margin over the last 120 kyr: Surface and subsurface paleoceanography, Paleoceanography, 17, 1055, doi:10.1029/2001PA000650, 2002. 586

Kienast, M., Kienast, S., Calvert, S., Eglinton, T., Mollenhauer, G., François, R., and Mix, A.: Eastern Pacific cooling and Atlantic overturning circulation during the last deglaciation, Nature, 443, 846–849, doi:10.1038/nature05222, 2006. 568, 586

Kohfeld, K., Le Quere, C., Harrison, S., and Anderson, R.: Role of marine biology in glacial-interglacial CO_2 cycles, Science, 308, 74–78, doi:10.1126/science.1105375, 2005. 560, 561, 563

Landais, A., Lathiere, J., Barkan, E., and Luz, B.: Reconsidering the change in global biosphere productivity between the Last Glacial Maximum and present day from the triple oxygen isotopic composition of air trapped in ice cores, Global Biogeochem. Cy., 21, GB1025, doi:10.1029/2006GB002739, 2007. 574

Landais, A., Dreyfus, G., Capron, E., Masson-Delmotte, V., Sanchez-Goņi, M., Desprat, S., Hoffmann, G., Jouzel, J., Leuenberger, M., and Johnsen, S.: What drives the millennial and orbital variations of δ^{18}Oatm?, Quaternary Sci. Rev., 29, 235–246, 2010. 574

Leduc, G., Vidal, L., Tachikawa, K., Rostek, F., Sonzogni, C., Beaufort, L., and Bard, E.: Mois-

CPD
8, 557–594, 2012

Marine productivity response to Heinrich events: a model-data comparison

V. Mariotti et al.

ture transport across Central America as a positive feedback on abrupt climatic changes, Nature, 445, 908–911, doi:10.1038/nature05578, 2007. 568

Lenton, A., Codron, F., Bopp, L., Metzl, N., Cadule, P., Tagliabue, A., Le Sommer, J.: Stratospheric ozone depletion reduces ocean carbon uptake and enhances ocean acidification, Geophys. Res. Lett, 36, L12606, doi:10.1029/2006GB002739, 2009. 571

Lin, H., Lai, C., Ting, H., Wang, L., Sarnthein, M., and Hung, J.: Late Pleistocene nutrients and sea surface productivity in the South China Sea: A record of teleconnections with Northern Hemisphere events, Mar. Geol., 156, 197–210, 1999. 586

Mahowald, N. M., Yoshioka, M., Collins, W. D., Conley, A. J., Fillmore, D. W., and Coleman, D. B.: Climate response and radiative forcing from mineral aerosols during the last glacial maximum, pre-industrial, current and doubled-carbon dioxide climates, Geophys. Res. Lett., 33, doi:10.1029/2006GL026126, 2006. 563

Marti, O., Braconnot, P., Dufresne, J., Bellier, J., Benshila, R., Bony, S., Brockmann, P., Cadule, P., Caubel, A., Codron, F., de Noblet, N., Denvil, S., Fairhead, L., Fichefet, T., Foujols, M.-A., Friedlingstein, P., Goosse, H., Grandpeix, J.-Y., Guilyardi, E., Hourin, F., Idelkadi, A., Kageyama, M., Krinner, G., Levy, C., Madec, G., Mignot, J., Swingedouw, D., and Talandier, C.: Key features of the IPSL ocean atmosphere model and its sensitivity to atmospheric resolution, Clim. Dynam., 34, 1–26, 2010. 563

Mashiotta, T., Lea, D., and Spero, H.: Glacial-interglacial changes in Subantarctic sea surface temperature and [delta]^{18}O-water using foraminiferal Mg, Earth Planet. Sc. Lett., 170, 417–432, 1999. 567

Matsumoto, K., Sarmiento, J., and Brzezinski, M.: Silicic acid leakage from the Southern Ocean: A possible explanation for glacial atmospheric $p\mathrm{CO}_2$, Global Biogeochem. Cy., 16, 1031, doi:10.1029/2001GB001442, 2002. 560

McManus, J., Francois, R., Gherardi, J., Keigwin, L., and Brown-Leger, S.: Collapse and rapid resumption of Atlantic meridional circulation linked to deglacial climate changes, Nature, 428, 834–837, doi:10.1038/nature02494, 2004. 559

Menviel, L., Timmermann, A., Mouchet, A., and Timm, O.: Meridional reorganizations of marine and terrestrial productivity during Heinrich events, Paleoceanography, 23, PA1203, doi:10.1029/2007PA001445, 2008. 560, 571, 572, 573

Merkel, U., Prange, M., and Schulz, M.: ENSO variability and teleconnections during glacial climates, Quaternary Sci. Rev., 29, 86–100, 2010. 567

Mohtadi, M. and Hebbeln, D.: Mechanisms and variations of the paleoproductivity off north-

Discussion Paper | Discussion Paper | Discussion Paper | Discussion Paper |

ern Chile (24 degrees S–33 degrees S) during the last 40,000 years, Paleoceanography, 19, PA2023, doi:10.1029/2004PA001003, 2004. 586

Monnin, E., Indermuhle, A., Dallenbach, A., Fluckiger, J., Stauffer, B., Stocker, T., Raynaud, D., and Barnola, J.: Atmospheric CO_2 concentrations over the last glacial termination, Science, 291, 112–114, doi:10.1126/science.291.5501.112, 2001. 560

Nave, S., Labeyrie, L., Gherardi, J., Caillon, N., Cortijo, E., Kissel, C., and Abrantes, F.: Primary productivity response to Heinrich events in the North Atlantic Ocean and Norwegian Sea, Paleoceanography, 22, PA3216, doi:10.1029/2006PA001335, 2007. 559, 585

Oka, A., Abe-Ouchi, A., Chikamoto, M., and Ide, T.: Mechanisms controlling export production at the LGM: Effects of changes in oceanic physical fields and atmospheric dust deposition, Global Biogeochem. Cy., 25, GB2009, doi:10.1029/2009GB003628, 2011. 560

Otto-Bliesner, B. and Brady, E.: The sensitivity of the climate response to the magnitude and location of freshwater forcing: last glacial maximum experiments, Quaternary Sci. Rev., 29, 56–73, 2010. 567

Pailler, D. and Bard, E.: High frequency palaeoceanographic changes during the past 140 000 yr recorded by the organic matter in sediments of the Iberian Margin, Palaeogeography, Palaeoclimatology, Palaeoecology, 181, 431–452, 2002. 585

Pauly, D. and Christensen, V.: Primary production required to sustain global fisheries, Nature, 374, 255–257, doi:10.1038/374255a0, 1995. 558

Penaud, A., Eynaud, F., Turon, J., Blamart, D., Rossignol, L., Marret, F., Lopez-Martinez, C., Grimalt, J., Malaizé, B., and Charlier, K.: Contrasting paleoceanographic conditions off Morocco during Heinrich events (1 and 2) and the Last Glacial Maximum, Quaternary Sci. Rev., 29, 1923–1939, doi:10.1016/j.quascirev.2010.04.011, 2010. 569, 585

Pichevin, L., Reynolds, B., Ganeshram, R., Cacho, I., Pena, L., Keefe, K., and Ellam, R.: Enhanced carbon pump inferred from relaxation of nutrient limitation in the glacial ocean, Nature, 459, 1114–1117, 2009. 568, 586

Radi, T. and de Vernal, A.: Dinocysts as proxy of primary productivity in mid-high latitudes of the Northern Hemisphere, Mar. Micropaleontol., 68, 84–114, 2008. 585

Rasmussen, T., Thomsen, E., Troelstra, S., Kuijpers, A., and Prins, M.: Millennial-scale glacial variability versus Holocene stability: changes in planktic and benthic foraminifera faunas and ocean circulation in the North Atlantic during the last 60 000 years, Mar. Micropaleontol., 47, 143–176, doi:10.1016/S0377-8398(02)00115-9, 2002. 585

Romero, O.: Changes in style and intensity of production in the Southeastern Atlantic over the

last 70,000 yr, Mar. Micropaleontol., 74, 15–28, 2010. 585
Romero, O., Kim, J., and Hebbeln, D.: Paleoproductivity evolution off central Chile from the Last Glacial Maximum to the Early Holocene, Quaternary Res., 65, 519–525, doi:10.1016/j.yqres.2005.07.003, 2006. 586
Romero, O., Kim, J., and Donner, B.: Submillennial-to-millennial variability of diatom production off Mauritania, NW Africa, during the last glacial cycle, Paleoceanography, 23, PA3218, doi:10.1029/2008PA001601, 2008. 569, 585
Romero, O. E., Leduc, G., Vidal, L., and Fischer, G.: Millennial variability and long-term changes of the diatom production in the eastern equatorial Pacific during the last glacial cycle, Paleoceanography, 26, PA2212, doi:10.1029/2010PA002099, 2011. 586
Sachs, J. and Anderson, R.: Increased productivity in the subantarctic ocean during Heinrich events, Nature, 434, 1118–1121, doi:10.1038/nature03544, 2005. 586
Salgueiro, E., Voelker, A., De Abreu, L., Abrantes, F., Meggers, H., and Wefer, G.: Temperature and productivity changes off the western Iberian margin during the last 150 ky, Quaternary Sci. Rev., 29, 680–695, 2010. 574, 585
Schmittner, A.: Decline of the marine ecosystem caused by a reduction in the Atlantic overturning circulation, Nature, 434, 628–633, doi:10.1038/nature03476, 2005. 560, 571, 572, 573
Schmittner, A. and Galbraith, E. D.: Glacial greenhouse-gas fluctuations controlled by ocean circulation changes, Nature, 456, 373–376, doi:10.1038/nature07531, 2008. 560
Schmittner, A., Oschlies, A., Matthews, H., and Galbraith, E.: Future changes in climate, ocean circulation, ecosystems, and biogeochemical cycling simulated for a business-as-usual CO_2 emission scenario until year 4000 AD, Global Biogeochem. Cy., 22, GB1013, doi:10.1029/2007GB002953, 2008. 561
Schneider, B., Bopp, L., Gehlen, M., Segschneider, J., Frölicher, T. L., Cadule, P., Friedlingstein, P., Doney, S. C., Behrenfeld, M. J., and Joos, F.: Climate-induced interannual variability of marine primary and export production in three global coupled climate carbon cycle models, Biogeosciences, 5, 597–614, doi:10.5194/bg-5-597-2008, 2008. 559, 571
Schulte, S. and Müller, P.: Variations of sea surface temperature and primary productivity during Heinrich and Dansgaard-Oeschger events in the northeastern Arabian Sea, Geo-Mar. Lett., 21, 168–175, 2001. 569, 586
Steinacher, M., Joos, F., Frölicher, T. L., Bopp, L., Cadule, P., Cocco, V., Doney, S. C., Gehlen, M., Lindsay, K., Moore, J. K., Schneider, B., and Segschneider, J.: Projected 21st cen-

tury decrease in marine productivity: a multi-model analysis, Biogeosciences, 7, 979–1005, doi:10.5194/bg-7-979-2010, 2010. 559, 561, 571, 573, 574, 575

Swartz, W., Sala, E., Tracey, S., Watson, R., and Pauly, D.: The spatial expansion and ecological footprint of fisheries (1950 to present), PLoS One, 5, e15143, doi:10.1371/journal.pone.0015143, 2010. 575

Swingedouw, D., Bopp, L., Matras, A., and Braconnot, P.: Effect of land-ice melting and associated changes in the AMOC results in little overall impact on oceanic CO_2 uptake, Geophys. Res. Lett, 34, L23706, doi:10.1029/2007GL031990, 2007. 561

Swingedouw, D., Mignot, J., Braconnot, P., Mosquet, E., Kageyama, M., and Alkama, R.: Impact of freshwater release in the North Atlantic under different climate conditions in an OAGCM, J. Climate, 22, 6377–6403, doi:10.1175/2009JCLI3028.1, 2009. 559

Tagliabue, A., Bopp, L., Roche, D. M., Bouttes, N., Dutay, J.-C., Alkama, R., Kageyama, M., Michel, E., and Paillard, D.: Quantifying the roles of ocean circulation and biogeochemistry in governing ocean carbon-13 and atmospheric carbon dioxide at the last glacial maximum, Clim. Past, 5, 695–706, doi:10.5194/cp-5-695-2009, 2009. 560, 563

Takeda, S.: Influence of iron availability on nutrient consumption ratio of diatoms in oceanic waters, Nature, 393, 774–777, 1998. 562, 568

Taucher, J. and Oschlies, A.: Can we predict the direction of marine primary production change under global warming?, Geophys. Res. Lett., 38, L02603, doi:10.1029/2010GL045934, 2011. 558, 564, 570, 571, 573

Thomas, E., Booth, L., Maslin, M., and Shackleton, N.: Northeastern Atlantic benthic foraminifera during the last 45,000 years: changes in productivity seen from the bottom up, Paleoceanography, 10, 545–562, 1995. 585

Toggweiler, J., Russell, J., and Carson, S.: Midlatitude westerlies, atmospheric CO_2, and climate change during the ice ages, Paleoceanography, 21, PA2005, doi:10.1029/2005PA001154, 2006. 560

Valdes, P.: Built for stability, Nat. Geosci., 4, 414–416, 2011. 574

Vink, A., Rühlemann, C., Zonneveld, K., Mulitza, S., Hüls, M., and Willems, H.: Shifts in the position of the North Equatorial Current and rapid productivity changes in the western Tropical Atlantic during the last glacial, Paleoceanography, 16, 479–490, doi:10.1029/2000PA000582, 2001. 585

Voelker, A.: Global distribution of centennial-scale records for Marine Isotope Stage (MIS) 3: a database, Quaternary Sci. Rev., 21, 1185–1212, 2002. 559

Table 1. Data compilation of paleoproductivity changes in response to Heinrich Events (HEs). For each record and each event, we summarize the trend of the proxies for paleoproductivity by a certain number of "−" or "+" signs. Each "−" (resp. "+") corresponds to a sensor indicating a significant decrease (resp. increase) in EXP. We discriminate between significant and not significant trend in sensors by applying a simple test on each time series. We compare the trend of the first 500 yr following a dated HE to the mean and variance of the 3000 yr preceding this dated HE (resp. 2000 yr for the Younger Dryas, YD). If the value of the first 500 yr is higher (resp. lower) than the addition of the mean and the variance (resp. the difference between the mean and the variance) of the last 3000 yr, we consider it as a significant increase (resp. decrease). When there is not such a significant trend, we display an "x". Some records, while having a sufficient time resolution (less than 500 yr between two measurements), had no dated HEs or YD. Would we have discarded them, only 33 out of the 49 studies would have remained. We decided to keep them and to date the HEs and YD ourselves on the time series, taking as an onset for these events −13 kyr for YD, −18 kyr for HE1, −25 kyr for HE2, −30 kyr for HE3, −40 kyr for HE4, −46 kyr for HE5, −60 kyr for HE6, −70.5 kyr for HE7 and −90 kyr for HE8. As they are time dating error bars issues on paleo-data, we consider these results as exploratory hypotheses, and are waiting for a real timing of the events to be more confident with them. To differentiate them from the well dated results we added a "?" in front of the concerned results. For each record, we summarize the results of all HEs and YD in one "value": when we add all the "−" and "+", if we obtain one "−" (resp. "+"), we write one "−" (resp. "+"), if we obtain more than two "−" (resp. "+"), we write "−−" (resp. "++") and finally if we have an equal number of "−" and "+" (or only "x"), we write an "x" because we consider that the records does not give a significant trend.

CPD
8, 557–594, 2012

Table 1a.

Core	Region	Latitude	Longitude	Water depth (m)	YD	HE1	HE2	HE3	HE4	HE5	HE6	HE7	HE8	Global	References
North Atlantic Ocean															
MD95-2008	–	62.74	−3.99	1016		x			x					x	Nave et al. (2007)
ENAM33	NATL	61.26	−11.11	1217	−−	x	x	x	−−	−	x			−−	Rasmussen et al. (2002)
MD95-2014	NATL	60.58	−22.08	2397		x			−					−	Nave et al. (2007)
DS97-2P	NATL	58.93	−30.4	1685	−−−	−	x	−	−	−−−				−−	Rasmussen et al. (2002)
BOFS-14K	NATL	58.62	−19.44	1759	?−	?−	x	x						?−	Thomas et al. (1995)
SU90-16	NATL	58.22	−45.17	2100		+			−					x	Nave et al. (2007)
SU90-39	NATL	52.57	−21.93	3955		−−			x					−−	Nave et al. (2007)
BOFS-5K	NATL	50.69	−21.87	3547	−	−	−	−	−					−−	Thomas et al. (1995)
HU 91-045-094	NATL	50.2	−45.69	3448	−−	−−	−							−−	Radi and de Vernal (2008)
SU90-44	NATL	50.02	−17.1	4279		x			x					x	Nave et al. (2007)
SU92-03	NATL	43.2	-10.11	3005		−	x	−	−	−	−	x	−	−−	Salgueiro et al. (2010)
MD95-2027	NATL	41.74	−52.41	4112		−			−					−−	Nave et al. (2007)
MD95-2040	NATL	40.58	−9.87	2465	x	−	x	x	x	−	−	x	−	−−	Pailler and Bard (2002), Salgueiro et al. (2010)
SU90-03	NATL	40.05	−32	2475		x			x					x	Nave et al. (2007)
MD95-2042	NATL	37.75	−10.17	3146	x	−−	−	−	x	−	x	−	−	−−	Pailler and Bard (2002), Salgueiro et al. (2010)
OCE326GGC6	NATL	33.69	−57.58	4541	x	x								x	Gil et al. (2009)
MD04-2805 CQ	MAU	34.51	−7.02	859	+	x	x							+	Penaud et al. (2010)
GeoB5546-2	MAU	27.53	−13.73	1070	x	+	x	x	+	x				++	Holzwarth et al. (2010)
GeoB7926-2	MAU	20.22	−18.45	2500	+	x								+	Romero et al. (2008)
M35003-4	–	12.08	−61.25	1299	−−	−−	−−	−−	−−	−−	x			−−	Vink et al. (2001)
PL07-39PC	–	10.7	−64.94	790	−	?−								−	Dean (2007)
PL07-57PC	–	10.68	−64.96	815	+									+	Hughen et al. (1996)
South Atlantic Ocean															
GeoB1706-2	BEN	−19.56	11.18	980	?x	?x	?+	?x	?−−	?−	?+			?−	Romero (2010)
GeoB1711-4	BEN	−23.32	12.38	1967	?−	?x	?+	?−	?−	?−−	?x			?−	Romero (2010)
GeoB3606-1	BEN	−25.47	13.08	1785	?x	?−	?x	?x	?x	?x	?−			?−	Romero (2010)

Table 1b.

Core	Region	Latitude	Longitude	Water depth (m)	YD	HE1	HE2	HE3	HE4	HE5	HE6	HE7	HE8	Global	References
Indian Ocean															
Core 136 KL	IND	23.12	66.5	568	?–	–	–	– – –	–	–	– –			– –	Schulte and Müller (2001)
Core 905	IND	10.77	51.95	1586	– – –	– –	– –	– –	– –	– – –	x			– –	Ivanochko et al. (2005)
North Pacific Ocean															
ODP 887	–	54.37	−148.45	3647	?x	?x								?x	Galbraith et al. (2007)
ODP 882	–	50.35	167.58	3300	?+	?x								?+	Galbraith et al. (2007)
W87-09-13PC	–	42.12	−125.75	2712	?– –	x	x	x						?– –	Kienast et al. (2002)
ODP 1019	–	41.68	−124.93	980	–	?–								–	Dean (2007)
MD02-2519	–	22.51	−106.65	955	?x	?–								?–	Arellano-Torres et al. (2011)
Core 17940-2	–	20.12	117.38	1727		x	x	x	x					x	Lin et al. (1999)
Core 17950-2	–	16.09	112.9	1865		x	x	+	x	+	x			++	Lin et al. (1999)
MD02-2524	–	12.01	−87.91	863	?x	?–								?–	Arellano-Torres et al. (2011)
MD02-2529	–	8.21	−84.12	1619	x	x	x	x	x	– –	– –	?– –		– –	Romero et al. (2011)
East Equatorial Pacific Ocean															
ODP 202 Core 1240	EEP	0.02	−86.46	2921	?x	?++	?– –							?x	Pichevin et al. (2009)
Core ODP 1240	EEP	0.02	−86.46	2921	?–	?+								?x	Arellano-Torres et al. (2011)
ODP site 1240	EEP	0.02	−86.46	2921	?x	?+								?+	Calvo et al. (2011)
ME0005A-24JC	EEP	0.02	−86.46	2941		+								+	Kienast et al. (2006)
ME0005A-24JC	EEP	0.02	−86.46	2941					++	++	+			++	Dubois et al. (2011)
South Pacific Ocean															
GeoB7112-5	–	−24.03	−70.82	2507	?– –									?–	Mohtadi and Hebbeln (2004)
GeoB7139-2	–	−30.20	−71.98	3267	?x	?x	?– –	?x						?–	Mohtadi and Hebbeln (2004)
GeoB3302-1	–	−33.22	−72.09	1498		?– –	?x	?+						?–	Mohtadi and Hebbeln (2004)
GeoB3359-3	–	−35.22	−72.81	678	?+	?x								?+	Romero et al. (2006)
Southern Ocean															
MD97-2120	–	−45.53	174.93	1210	+	+	x	x	x	++	+			++	Sachs and Anderson (2005)
TN057-13-4PC	–	−53.2	5.1	2850		++								++	Anderson et al. (2009)
E27-23	NZL	−59.62	155.24	3182		++								++	Anderson et al. (2009)
NBP9802-6PC	NZL	−61.8	−170	3245		++								++	Anderson et al. (2009)

CPD
8, 557–594, 2012
Marine productivity response to Heinrich events: a model-data comparison
V. Mariotti et al.

Table 2. Definition and characteritics of the regions chosen for the data-model comparison.

Region	Description	Box	Area (10^{12} m^2)	EXP(GLA) (PgC yr^{-1})	ΔEXP (PgC yr^{-1}) (%)
NATL	North Atlantic	30° N–60° N ; 70° W–10° W	13.89	0.61	−0.27 (−44)
MAU	Mauritanian Coast	15° N–35° N; 20° W–0° W	1.460	0.045	−0.026 (−58)
BEN	Benguela Coast	30° S–0° S; 5° E–15° E	2.629	0.14	−0.092 (−66)
IND	Northern Indian	10° S–30° S; 45° E–100° E	17.56	0.38	−0.18 (−47)
EEP	Eastern Equatorial Pacific	5° S–5° N; 130° W–80° W	6.676	0.31	0.0064 (+2)
NZL	South of New Zealand	70° S–55° S; 150° E–170° W	3.051	0.083	0.0053 (+6.4)
SEP	South East Pacific	65° S–40° S; 170° W–90° W	8.656	0.22	−0.037 (−17)
GLO	Global Ocean	–	341.5	9.3	−1.5 (−16)

CPD
8, 557–594, 2012

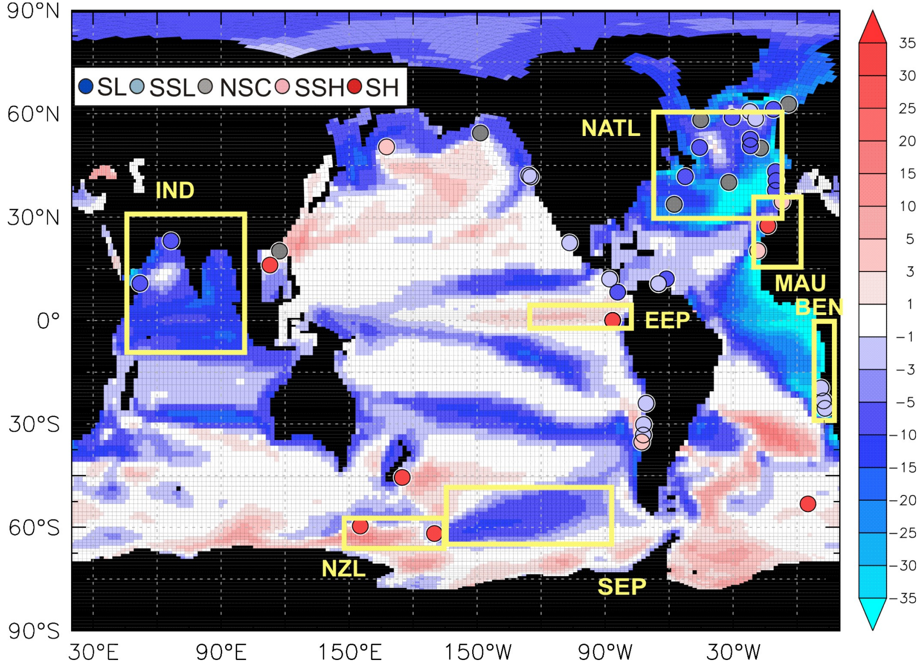

Fig. 1. FWF-GLA export differences (in g m^{-2} yr^{-1}) averaged for the simulated years 350–399 (filled field), alongside paleoproductivity changes during Heinrich events compared to glacial mean state reconstructed from our compilation (points). Dark and light blue points represent significantly lower (SL) and slightly significantly lower (SSL) export production respectively (equivalent to "−−" and "−" or "?−" in Table 1). Dark and light red points represent significantly higher (SH) and slightly significantly higher (SSH) export production respectively (equivalent to "++" and "+" or "?+"). The grey points represent no significant change (NSC) (equivalent to "x" or "?x").

CPD
8, 557–594, 2012

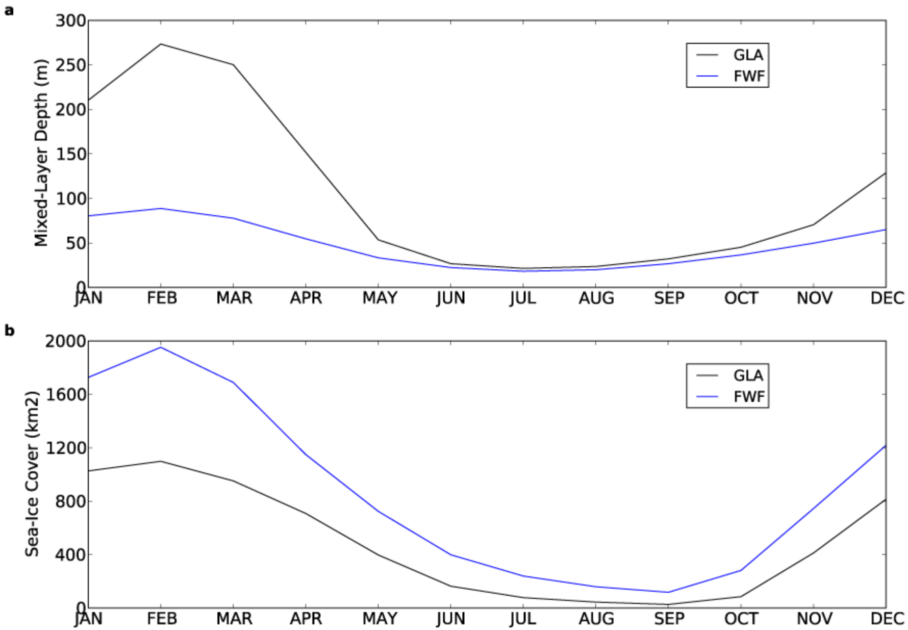

Fig. 2. NATL area **(a)** mixed-layer depth (in meters) and **(b)** sea-ice cover (in km^2) seasonal cycle for FWF (blue) and GLA (black) simulations, averaged for the simulated years 350–399.

CPD
8, 557–594, 2012

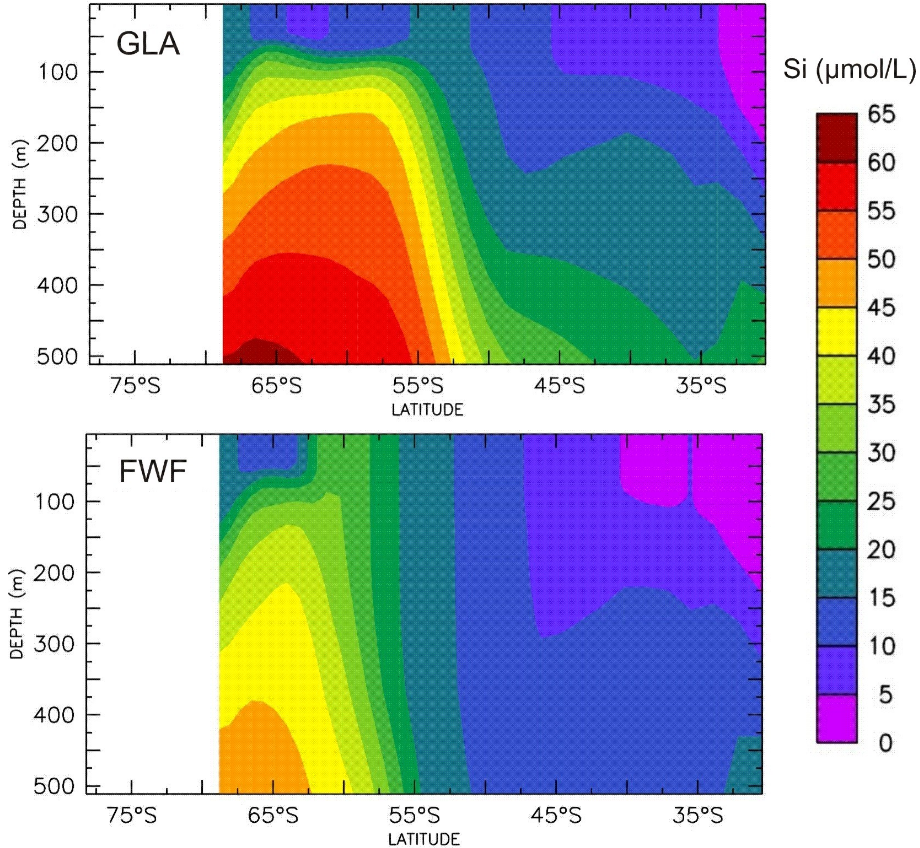

Fig. 3. Acid silicic concentration in NZL area for GLA and FWF runs (longitudinal transect at 152° East averaged on months of August and September for the last 50 yr of each simulation).

CPD
8, 557–594, 2012

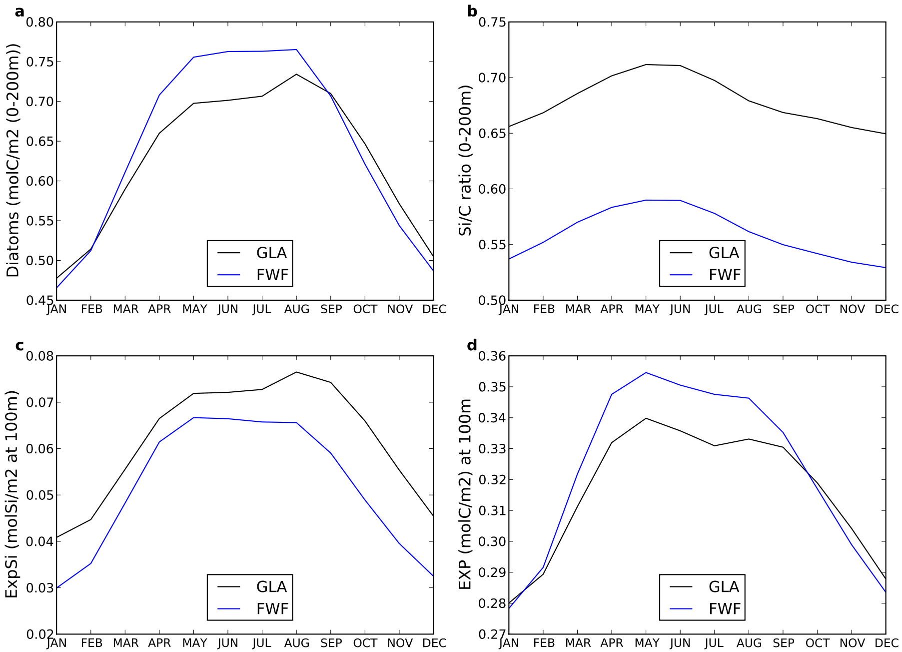

Fig. 4. Average on the EEP area (simulated years 350–399) of **(a)** diatom concentration (in molC m^{-2} averaged on the first 200 m of the water column), **(b)** Si/C ratio (also averaged on the first 200 m of the water column), **(c)** silica export (ExpSi) at 100 m (in molSi m^{-2}) and **(d)** EXP (export production) at 100 m (in molC m^{-2}).

CPD
8, 557–594, 2012

Marine productivity response to Heinrich events: a model-data comparison

V. Mariotti et al.

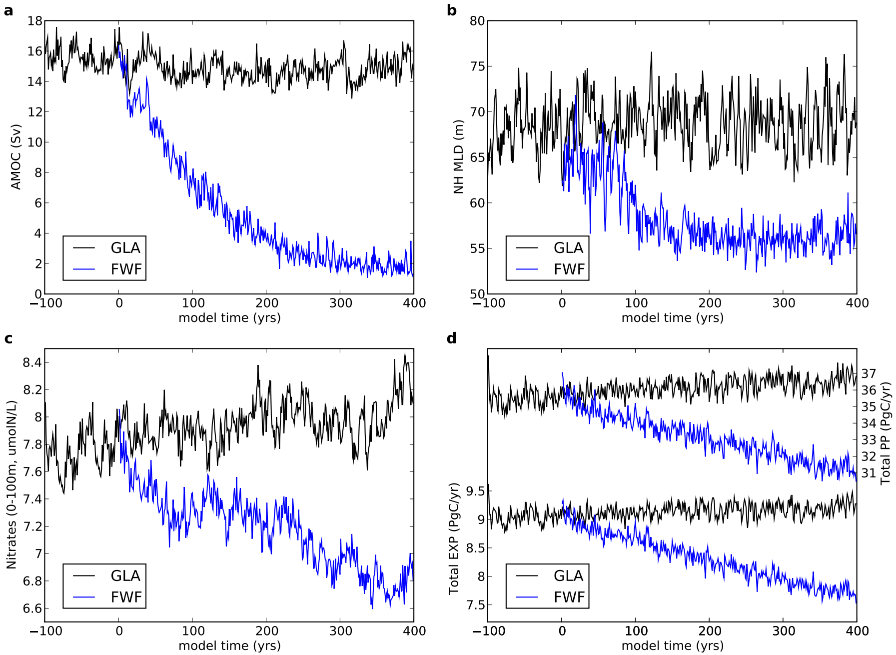

Fig. 5. **(a)** AMOC (Sverdrups, 1 Sverdrup = 10^6 m^{-3} s^{-1}), **(b)** globally averaged maximum northern hemisphere mixed-layer depth (m), **(c)** globally averaged nitrates concentration (µmol l^{-1}) and **(d)** globally averaged PP (primary productivity) and EXP (export production) for both simulations, GLA (black) and FWF (blue) (PgC yr^{-1}).

CPD
8, 557–594, 2012

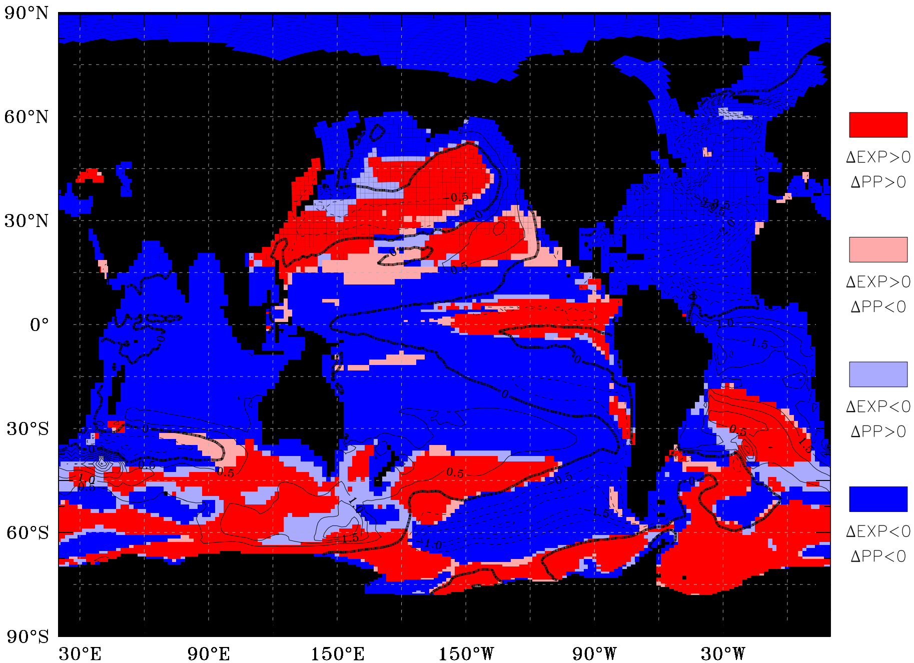

Fig. 6. Comparative change in PP (primary productivity) and EXP (export production) (with $\Delta X = \frac{X(\text{FWF})-X(\text{GLA})}{X(\text{GLA})}$, X averaged on simulated years 350–399) (filled field) and sea surface temperature anomaly (isolines each 0.5 degrees Celsius) for the simulated years 350–399.

CPD
8, 557–594, 2012

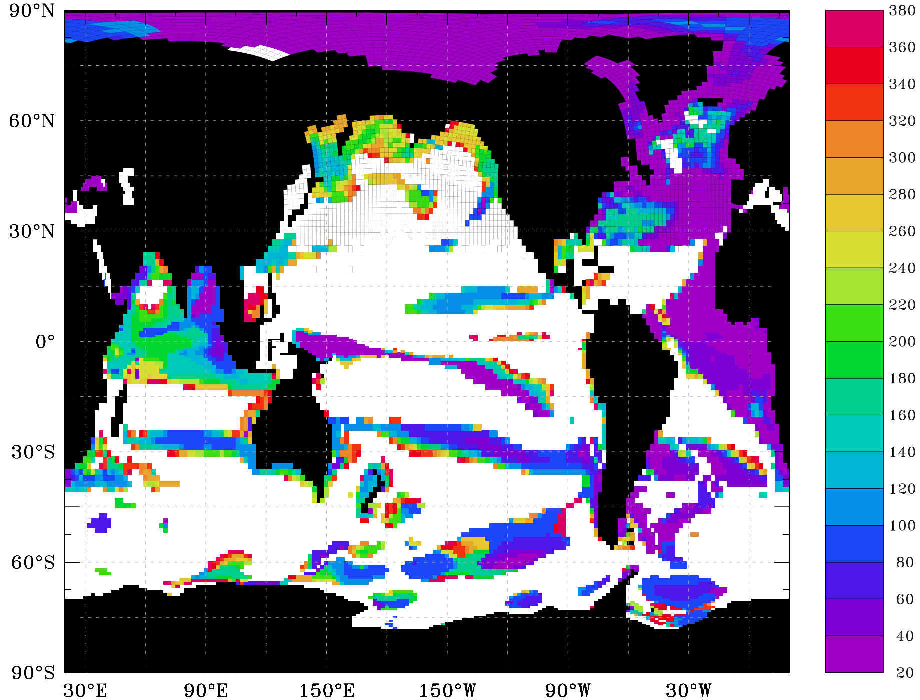

Fig. 7. FWF-GLA time response (in years) of EXP (export production): defined as the time after which half of the final signal (averaged on the simulated years 350–399) in EXP has been reached. We only considered regions where the final anomaly of EXP was more than 1 $gC\,m^{-2}\,yr^{-1}$ in absolute value: the white areas in the ocean do not have such an important anomaly in the end.

CPD
8, 557–594, 2012